Title

Multiphase Mechanism for the Production of Sulfuric Acid from SO2 by Criegee Intermediates Formed During the Heterogeneous Reaction of Ozone with Squalene

Journal

The Journal of Physical Chemistry Letters, 9(12)

ISSN

1948-7185

Authors

Heine, Nadja
Arata, Caleb
Goldstein, Allen H
et al.

Publication Date

2018-06-21

DOI

10.1021/acs.jpclett.8b01171

Peer reviewed

A Multiphase Mechanism for the Production of Sulfuric Acid from SO_2 by Criegee Intermediates Formed During the Heterogeneous Reaction of Ozone with Squalene

Nadja Heine[†], Caleb Arata[‡,§], Allen H. Goldstein[§], Frances A. Houle[†,], Kevin R. Wilson[†,*]*

[†]Chemical Sciences Division, Lawrence Berkeley National Laboratory, Berkeley, California, USA, [§]Department of Chemistry, University of California, Berkeley, California 94720, United States, [‡]Department of Environmental Science, Policy and Management and Department of Civil and Environmental Engineering, University of California, Berkeley, California, USA

*Corresponding Authors: krwilson@lbl.gov, fahoule@lbl.gov

ABSTRACT: Here we report a new multiphase reaction mechanism by which Criegee Intermediates (CI), formed by ozone reactions at an alkene surface, convert SO_2 to SO_3 to produce sulfuric acid; a precursor for new particle formation (NPF). During the heterogeneous ozone reaction, in the presence of 220 ppb SO_2, an unsaturated aerosol (squalene) undergoes rapid chemical erosion, which is accompanied by NPF. A kinetic model predicts that mechanism for chemical erosion and NPF originate from a common elementary step (CI + SO_2) that produces both gas phase SO_3 and small ketones. At low relative humidity (RH = 5%), 20% of the aerosol mass is lost, with 17% of the ozone-surface reactions producing SO_3. At RH = 60%, the aerosol shrinks by 30% and the yield of SO_3 is < 5%. This multiphase formation mechanism of H_2SO_4 by CIs is discussed in the context of indoor air quality and atmospheric chemistry.

TOC GRAPHIC

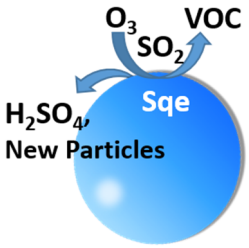

Surface reactions of gas phase oxidants (e.g. O_3 and OH) and organic molecules play a substantial role in the chemical erosion and molecular weight growth at indoor surfaces and in the atmosphere (e.g. aerosols).(1-7) Although major oxidation pathways of many organic molecules are known in the gas phase and to a large extent in the condensed phase, there remains considerable uncertainty in understanding the multiphase pathways (e.g. gas + liquid) of transient intermediates, such as free radicals and Criegee Intermediates (CI). Key questions include whether reactions at aerosol and other surfaces are a source of gas phase radicals or CIs, or whether these intermediates formed at an interface can initiate chemistry with trace gas species.(7-9) Here we examine how CIs, formed by ozonolysis reactions at an organic interface, can oxidize SO_2 to SO_3, which then reacts rapidly with water vapor to form H_2SO_4.

SO_2 is an anthropogenic pollutant that, when oxidized to H_2SO_4, plays a central role in acid rain and new particle formation (NPF) in the troposphere.(10-13) Key gas phase reaction pathways (e.g. OH + SO_2) that oxidize SO_2 to H_2SO_4 are well known. Recently, it was shown that the gas phase reaction of CIs with SO_2 are many orders of magnitude faster than with H_2O. (14-18) Huang *et al.* demonstrated that stabilized secondary CIs react with SO_2 at nearly the gas kinetic-limit, and only slowly with water vapor, leading to the survival of these intermediates even at high relative humidity (RH).(18) There are also known heterogeneous pathways that convert gas phase SO_2 to sulfate on mineral surfaces, marine aerosol and droplets (i.e. acid rain).(19-21) Li *et al.* showed

that while gas phase SO_2 reacts only very slowly with O_3 and H_2O, sulfur dioxide adsorbed on $CaCO_3$ surfaces can be rapidly converted to sulfuric acid.(22-23) In comparison, little is known about the heterogeneous conversion of SO_2 to SO_3 by CIs produced from surface alkene reactions with O_3.

Here we examine the reaction between an aerosol comprised of squalene (Sqe, a $C_{30}H_{50}$ branched alkene with 6 C=C bonds) and gas phase ozone as a function of both relative humidity and trace amounts of SO_2 (Scheme 1) to explore viable pathways for the heterogeneous production of SO_3. Sqe accounts for ≤12% of human skin oil, and is found on many indoor surfaces due to frequent skin shedding.(24-26) Sqe reacts rapidly with ozone, and constitutes the main indoor sink for this oxidant. Gas phase products from this reaction are commonly observed in indoor air and are known respiratory irritants.(24, 27-29) Thus ozone oxidation of Sqe on indoor surfaces and human skin is a key reaction for indoor air chemistry and thus air quality, and it is therefore important to better understand the reaction mechanisms and products, especially at relevant oxidant and trace gas concentrations.

To study this reaction a flow tube reactor is combined with an aerosol mass spectrometer, described in Heine *et al.* and summarized in the Supplementary Information (SI).(30) This approach is used to quantify the kinetic decay of Sqe, the formation kinetics of major reaction products and the change in particle size as a function of ozone exposure ($[O_3]$ x time).

The experimental observations presented here are compared to predictions from a previously developed and validated kinetic model implemented in Kinetiscope, extended to include SO_2 chemistry.(31) The model already successfully explains the molecular mechanism for chemical erosion observed during the heterogeneous ozonolysis of Sqe aerosol (without SO_2).(30)

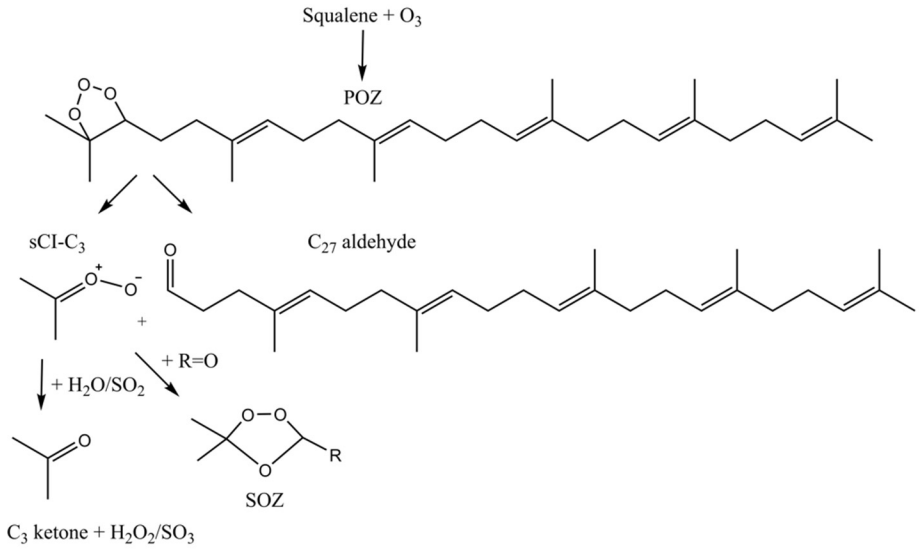

Scheme 1. A simplified Sqe ozonolysis reaction scheme showing how H_2O and SO_2 participate in the formation pathways of the major carbonyl and secondary ozonide (SOZ) products.

The model captures multiphase processes including the adsorption of O_3 to the particle surface and the evaporation of volatile reaction products. Scheme 1 summarizes the main product formation channels, and **R1**, **2a**, **3**, **4** and **6** in Table 1 show the elementary steps, stoichiometry and rate constants. O_3 adds to 1 of the 6 double bonds, forming a primary ozonide (POZ), which decomposes into a carbonyl and a zwitterion, the Criegee Intermediate (CI). The bond location of the ozone attack produces CIs and carbonyl co-products with distinct carbon chain lengths. The presence of a branched methyl group on the C=C bond means that decomposition of the POZ is asymmetric, forming either a CI on a primary carbon atom (pCI) and ketone co-product or a CI on a secondary carbon (sec-CI) and an aldehyde (see Scheme 1 and Fig. S1 for detailed reaction mechanism).

Table 1. Reaction scheme and rate constants for stochastic simulations.

No.	Reaction step	Rate constant	Notes
	O_3_gas → O_3_adsorbed	1.97 s^{-1}	a)
R1	Sqe + O_3 → sec/p-CI + R=O	$1.25 \cdot 10^{-15}$ cm^3 $molec^{-1}$ s^{-1}	b),c)
R2a	CI + H_2O → R=O + H_2O_2	5.14 s^{-1}	d)
R2b	CI + SO_2 → R=O + SO_3	58.4 s^{-1}	e)
R3	CI + R=O → SOZ	$6.7 \cdot 10^{-19}$, $1.3 \cdot 10^{-18}$ cm^3 $molec^{-1}$ s^{-1}	f)
R4	CI → R(O)OH, HOR=O	5 s^{-1}	Ref.(32) g)
R5	CI → ·R=O + OH·		h)
R6	CI + O_3 → R=O	$4 \cdot 10^{-13}$ cm^3 $molec^{-1}$ s^{-1}	Ref.(33) i)
R7	SO_3 → SO_3_gas	$2.8 \cdot 10^{9}$ s^{-1}	j)

a) Rate coefficient depends on O_3 sticking coefficient ($1.8 \cdot 10^{-4}$)(34), particle diameter (d) and average [O_3]; here: d=300 nm, [O_3]=$2.81 \cdot 10^{13}$ molecules cm^{-3}. b) Either a pair of aldehyde and secondary Criegee intermediate (sec-CI) or ketone and primary CI (pCI) can be formed. In previous work we showed that the ratio of this fragmentation is 1:9 (pCI:sec-CI).c) Experimental second-order rate constant taken from Ref. (35). d) Treated as pseudo first order where [H_2O] = 3-60% (shown for 3%), k = $1 \cdot 10^{-14}$ cm^3 $molecules^{-1}$ s^{-1} (from Ref. (15)) and the dimensionless Henry's law constant is $2.6 \cdot 10^{-2}$, which applies to solubility of water in aliphatic compounds with comparable viscosity.(36) e) Treated as pseudo first order where [SO_2] = 220 ppb, k = $3.9 \cdot 10^{-11}$ cm^3 $molecules^{-1}$ s^{-1} (from Ref. 15) and the dimensionless Henry's law constant of $2.7 \cdot 10^{-1}$, for the solubility of SO_2 in aliphatic compounds with comparable viscosity.(37) f) Constrained by calculation and experiment see Heine *et al.*(30) for details. g) Sensitivity tests of this rate coefficient are shown in Fig. S7 h) R5 was not considered in the model, see SI and Ref. (30) for details. i) Sensitivity tests of this rate coefficient are shown in Fig. S8 j)Evaporation rate constant calculated from SO_3 vapor pressure (2.07 bar).(38) For details see text and Ref. (39).

Reaction of the CI with either water or a carbonyl (Scheme 1) leads to the formation of the two main product classes (carbonyls and secondary ozonides, SOZ respectively).(30) At solid alkene interfaces, Karagulian et al. proposed an alternative mechanism in which O_3 and H_2O directly react with a long lived POZ to form carbonyl and SOZ products.(40) In Ref. (30) we show, however, that the observed carbon number distribution of SOZs, as well as product evolution and volume change of the aerosol as a function of RH, are due to the formation of mainly sec-CI and aldehyde coproducts. The sec-CIs are small (C_3, C_8, and C_{13}), and react with water to form ketones that erode the particle surface. This process is responsible for the substantial decrease (by ~20%) in aerosol size (i.e. chemical erosion) at RH = 60% as shown in Fig. 1 and Ref.(30) To capture the effect of adding SO_2, a reaction step was added to the model(30): CI + SO_2 → carbonyls + SO_3

(**R2b** in Table 1). SO_2 is assumed to react in the bulk and its concentration is given by its Henry's law solubility. The pseudo first order rate coefficient is calculated using the dimensionless Henrys law constant, [SO_2] and the SO_2 + CI gas phase rate constant measured for the reaction of SO_2 with CH_2OO.(14, 41-43)

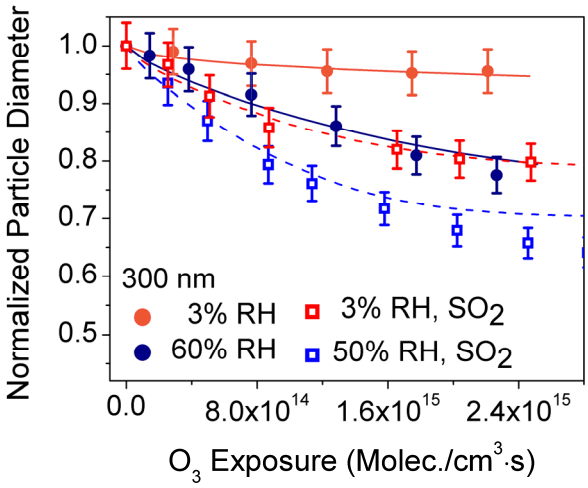

Figure 1. Normalized particle diameter of size-selected (300 nm) Sqe particles without (circles) and with (squares) 220 ppb SO_2 as function of RH. Solid and dashed lines represent model predictions. Error bars are estimated from the SMPS bin width and replicate measurements.

Fig. 1 presents experimental and model simulation results that show that the addition of 220 ppb ($5.6 \cdot 10^{12}$ molec./cm^3) of SO_2 to the flow reactor produces a substantial change in aerosol diameter. This provides clear evidence that, similar to water, SO_2 produces chemical erosion. The quantity of aerosol mass lost as a function of ozone exposure is much larger for SO_2 than H_2O. Under SO_2-free conditions the particle diameter shrinks by ~5% at RH = 3% increasing to ~20% at RH = 60%. Addition of only 220 ppb SO_2 under dry conditions (RH = 3%) leads to a ~20% decrease in particle diameter, equivalent to what is observed at RH = 60% without SO_2. As shown in Scheme 1, the

reaction steps involved are analogous for SO_2 and H_2O. SO_2 reacts with CIs to form carbonyls and SO_3.(11, 13, 32, 44-47) The CI + H_2O reaction also produces carbonyls, albeit with a different co-product, H_2O_2. The substantial difference in [SO_2] and [H_2O] that is needed to achieve equivalent levels of chemical erosion suggests that the overall CI + SO_2 reaction rate constant is substantially greater than that of the analogous CI + H_2O reaction.

As shown in Fig. S2, the presence of SO_2 does not alter the decay kinetics of Sqe as a function of ozone exposure and RH. This shows that the formation of SO_3 (or the presence of gas phase SO_2) does not accelerate the consumption rate of Sqe through secondary or chain propagation reactions. Also, adding SO_2 does not alter the identity of the major ozonolysis products (aldehydes and SOZs) previously observed(30) and shown in Fig. S3. No evidence is found for new products such as organosulfates, as was recently reported for heterogeneous SO_2 + alkene reactions.(48)

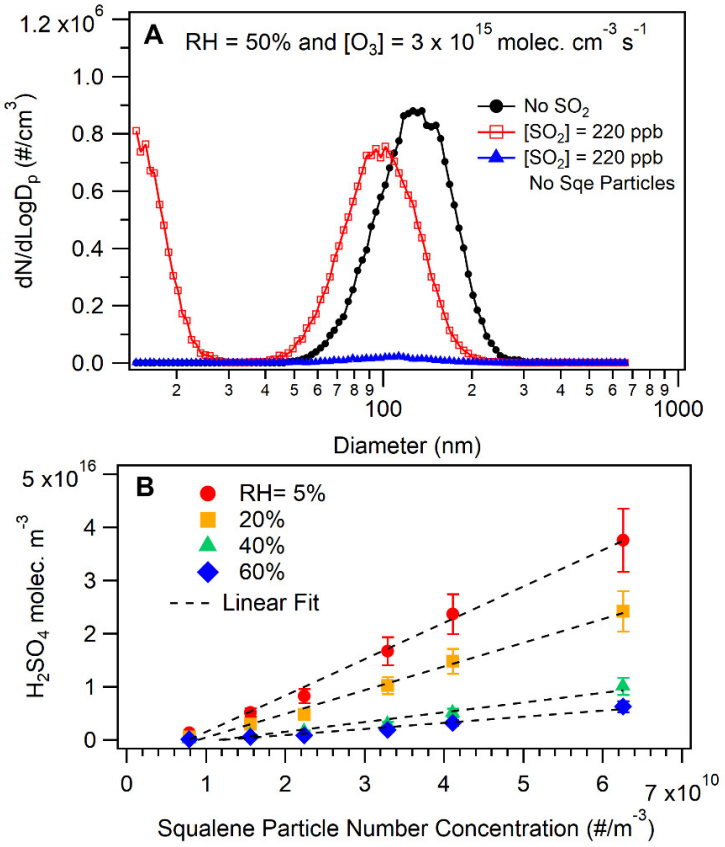

Figure 2. a) Particle size distribution (normalized concentration as function of particle diameter), with and without Sqe ($d \sim 180$ nm) and SO_2 showing chemical erosion and NPF. Particle size measurements are shown for RH = 50% and $[O_3] = 3 \cdot 10^{15}$ molec./cm^3·s. Black circles show Sqe-only measurements, red squares show results from the addition of SO_2. Blue triangles depict measurements with SO_2, but without Sqe. b) H_2SO_4 concentration as a function of Sqe particle number concentration and RH at $[O_3] = 1.2 \cdot 10^{16}$ molec./cm^3·s.

Instead of forming new molecular products, new particle formation (NPF) is observed. Fig. 2a shows a typical size distribution with and without Sqe aerosol and SO_2 at RH = 50% and $[O_3] = 3 \cdot 10^{15}$ molec./cm^3·s. The Sqe particle distribution is centered at 180 nm without SO_2. With 220 ppb SO_2 there is a decrease in the average Sqe aerosol size distribution (due to chemical erosion discussed above), which is accompanied by a new mode at ~14.6 nm that is assigned to NPF. Additional measurements have been carried out using a nano DMA to cover a size range specific

to the newly formed particles as shown in Fig. S4. The chemical identity of the new particles is established as follows. NPF only occurs in the presence of Sqe aerosol, O_3 and SO_2 together, and disappears when Sqe is removed from the reactor. Furthermore, at each RH there is a linear increase (Fig. 2b) in the quantity of new particles that depends upon the total number of Sqe aerosol introduced into the flow reactor. These observations show that the NPF mode observed in Fig. 2a is from heterogeneous reactions (in the presence of O_3) and not from purely gas phase reactions (e.g. $SO_2 + O_3$). The primary new product formed from SO_2 reacting with sec-CI is SO_3. Since SO_3 reacts rapidly with water to make H_2SO_4, and H_2SO_4 is known to nucleate to form particles, we assign the new mode to small H_2SO_4 particles.(49-53)

Shown in Fig. 2b is the measured NPF mass/m^3 (expressed in molecular units, H_2SO_4) as a function of Sqe particle number and RH. In addition to the increase in NPF mass and diameter with increasing [O_3] (shown in Fig. S4), there is a clear increase in the quantity of H_2SO_4 when the RH is decreased from 60% to 5%.

As noted above, **R2b** is assumed to occur in the particle bulk. An alternative is that SO_2 only reacts at the particle surface. In this case the reaction rate would be governed by the SO_2 collision frequency, sticking probability and particle surface area. Simulations of this scenario, which include the range of reported CI + SO_2 rate coefficients, shown in Fig. S6, predict a much smaller change in particle diameter than is observed even if a sticking probability of 1 is assumed.(17-18) This validates our assumption that the CI + SO_2 reaction occurs mainly in the interior of the aerosol.

After SO_3 is formed, it can react with dissolved water in the particle or evaporate since it has a substantial vapor pressure. An evaporation step is included in the model (**R7**) using the vapor

pressure of SO_3(38) to compute an evaporation coefficient (k_{evap} = $2.8 \cdot 10^9$ s^{-1}) as described in Ref.(54). The pseudo first order reaction rate constant for SO_3 with dissolved water at RH =60% is computed to be 12.3 s^{-1} using the Henry's law constant for water shown in Table 1 and the bimolecular $SO_3 + H_2O$ rate coefficient ($1.2 \cdot 10^{-15}$ molec./$cm^3 \cdot s^1$).(49) This rate constant is ~$2.2 \cdot 10^8$ times slower than that for evaporation, suggesting that once formed, SO_3 desorbs into the gas phase rather than reacting with aerosol water. This was confirmed by running simulations with and without the particle phase $SO_3 + H_2O$ reaction step, confirming that it is kinetically insignificant. Once SO_3 desorbs into the gas phase, it rapidly reacts with water vapor to form sulfuric acid. The estimated gas phase lifetime of SO_3 under our reaction conditions is short (e.g. ~2 ms at RH = 60%).

The model, including the elementary SO_2 steps described above, quantitatively predicts the experimental Sqe decay (Fig. S2), the carbonyl formation kinetics (Fig. S5) and the decrease in aerosol diameter (Fig. 1) as a function of ozone exposure and RH. The model fails to capture the RH dependence of the SOZs formation kinetics (Fig. S5). This is a deficiency found in our previous study, and it reflects gaps in our understanding of how SOZ reacts with [H_2O].(30)

The model confirms that the chemical erosion at RH = 3% is driven mainly by the SO_2 + CI reaction, whose rate constant is ~4000 times larger than CI + H_2O. Both reactions form small molecular weight ketones with high volatility, as shown in Scheme 1 and Fig. S1. With increasing RH, the CI + H_2O reaction grows in importance, providing a second path for chemical erosion of the aerosol. By use of markers in the simulations, the model allows us to track products specific to either of those reactions. At RH=3%, 9.3% of acetone comes from CI + SO_2 and only 0.9% from CI + H_2O, while at RH = 60%, 12% of acetone is formed via the water reaction vs. 9.3% from SO_2.

From the slope of the linear fit to the results shown in Fig. 2b, the number of H_2SO_4 molecules produced per squalene particle at $[O_3] = 1.2 \cdot 10^{16}$ molec./cm^3·s can be estimated. The experimental yield of H_2SO_4 per particle can then be used to compute to the number of H_2SO_4 molecules produced per O_3 collision with the particle surface. This is shown in Fig. 3, and compared to the model predictions. At RH = 5% the model and experiment are in reasonable agreement with a H_2SO_4 (SO_3) production probability of $\sim 3 \cdot 10^{-5}$ per O_3 *collision*. As shown in Fig 3, this corresponds to a ~17% probability of producing a H_2SO_4 (SO_3) molecule per O_3 *reaction*, since the O_3 sticking probability is rather small, $1.8 \cdot 10^{-4}$ (a value constrained in the O_3-Sqe simulations(30)). As RH increases, the CI + H_2O reaction becomes more important, decreasing the reactive yield of SO_3 to less than 5% per O_3 reaction at RH = 60%.

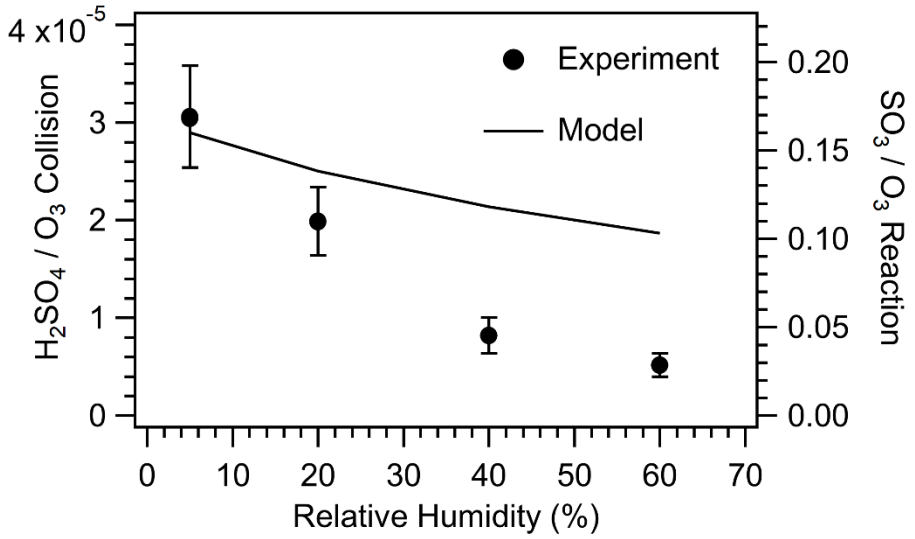

Figure 3. Measured (circles) and predicted (line) concentration of sulfuric acid per O_3 collision (left axis) and reactivity to produce SO_3 in the aerosol particle (right axis) as a function of RH. Error bars are estimated from the error of the linear fit in Fig. 2b and the uncertainty of $[O_3]$.

While the model captures the overall trend of decreasing SO_3 yield with increasing RH, the predictions increasingly deviate from experiment at higher RH (i.e. by a factor of ~2 at RH = 60%). There are aspects of the model that can lead to over prediction of H_2SO_4. As discussed in previous

work(30), the model has a sec-CI to SOZ path that is too fast at higher RH. This channel would result in SO_3 concentrations that are too high. The model also lacks sinks (e.g. flow tube walls) for H_2SO_4 that might become more important under wet conditions. It could be feasible to assess the importance of these possibilities by predicting NPF, which involves nucleation and surface catalyzed growth.(22, 55-58) These processes are complex to integrate into the simulation framework used here, however, and are beyond the scope of this work.

We considered two other possible pathways for NPF. First, we cannot entirely rule out that some fraction of C_3, C_8, and C_{13} sec-CI themselves, once formed in the aerosol, could evaporate and react in the gas phase with SO_2. The particle phase [sec-CI] directly controls SOZ formation, and indirectly the population of aldehydes in the aerosol as shown by Heine *et al.*(30) If their evaporation were significant the RH dependence of all the major products as well as the volume loss from the particle would be substantially altered from what is observed. Second, it is possible that the C_8 and C_{13} ketones (containing 1 and 2 C=C respectively), which are responsible for chemical erosion, could further react in the gas phase with O_3 forming CIs that subsequently react with gas phase SO_2 to form SO_3. If this were the case we would expect NPF to be actually enhanced at high relative humidity where the concentration of these products is the highest. However, this is not what is observed in Fig. 3, where the SO_3/H_2SO_4 yield is the highest under dry conditions.

Given these considerations, the agreement between experiment and model appears reasonable, and provides evidence that NPF occurs via the following multiphase mechanism: *SO_3, produced by the CI + SO_2 reaction in the aerosol, evaporates from the particle to react with water vapor to initiate NPF*.

Although our experiments use a simplified single component aerosol as proxy for the more complex unsaturated mixed aerosol or species on indoor surfaces and in the atmosphere, the results point to a new multiphase mechanism for SO_2 oxidation, which is expected to be general for similar unsaturated compounds and mixtures. Our results show that the oxidation of SO_2 via Criegee chemistry competes with water vapor and leads to an enhanced chemical erosion of the Sqe aerosol, as well the formation of sulfuric acid. The elementary reaction steps were reproduced with a kinetics model, which could also quantitatively predict the amount of H_2SO_4 formed during the reaction.

The results of our study indicate that Sqe aerosol ozonolysis may have an impact on production pathways for new particles under both indoor and atmospherically relevant RH, SO_2 and O_3 concentrations. This pathway is enhanced under dry conditions, in which more SO_2 is oxidized to SO_3 (the precursor of H_2SO_4). Furthermore, the significant chemical erosion of the particles, which is even more pronounced under humid conditions, leads to an enhanced formation of volatile organic compounds, which may contribute to the formation of secondary organic aerosol (SOA) in the atmosphere. Enhanced SOA formation has been previously associated with sulfate-rich conditions, however, the underlying mechanism remained poorly understood.(7)

Our results suggest that in highly polluted and dry regions, such as low income homes in Africa where solid fuels are commonly burned for cooking and heating,(59-60) the formation of sulfuric acid from multiphase chemistry may constitute an additional and so far unknown source of respiratory irritants indoors. Sqe ozonolysis in SO_2 polluted homes may therefore furthermore increase the health risks that are already associated with high SO_2 by enhanced formation of the main volatile ozonolysis products, acetone, 6-Methyl-5-hepten-2-one, geranyl acetone, next to sulfuric acid.

ASSOCIATED CONTENT

Supporting Information.

S1. Experimental and Modeling Methods: Detailed description of experimental setup for measuring the heterogeneous ozone kinetics and NPF. Further details about the simulation methods are described.

S2. Reaction Mechanism: Schematic of the full reaction mechanism used in the model simulations.

S3. Supporting Results: Experimental results including the reactive decay of Sqe, product mass spectra and kinetic evolution are presented. NPF heterogeneous nucleation curves are shown as a function of particle loading, ozone exposure, and RH.

S4. Modeling Scenarios to evaluate surface vs. bulk reaction for the CI + SO_2 elementary step. Sensitivity test for the isomerization rate constant (R4) and sensitivity test for the CI + O_3 rate constant (R6).

AUTHOR INFORMATION

Corresponding Author

*E-mail: krwilson@lbl.gov, fahoule@lbl.gov

Notes

The authors declare no competing financial interest.

ACKNOWLEDGMENT

This work is supported by the Department of Energy, Office of Science, Office of Basic Energy Sciences, Chemical Sciences, Geosciences, and Biosciences Division, in the Gas Phase Chemical Physics Program under Contract No. DE-AC02-05CH11231. This research used resources of the Advanced Light Source, which is a DOE Office of Science User Facility under contract no. DE-AC02-05CH11231. A.G. and C.A. are supported by the Alfred P. Sloan Foundation Chemistry of Indoor Environments program. N.H. thanks the Alexander-von-Humboldt Foundation for a post-doctoral research fellowship.

REFERENCES

(1) Ravishankara, A. R. Heterogeneous and Multiphase Chemistry in the Troposphere. *Science* **1997,** *276*, 1058-1065.

(2) Estillore, A. D.; Trueblood, J. V.; Grassian, V. H. Atmospheric Chemistry of Bioaerosols: Heterogeneous and Multiphase Reactions with Atmospheric Oxidants and Other Trace Gases. *Chem. Sci.* **2016,** *7*, 6604-6616.

(3) Donaldson, D. J.; Valsaraj, K. T. Adsorption and Reaction of Trace Gas-Phase Organic Compounds on Atmospheric Water Film Surfaces: A Critical Review. *Environ. Sci. and Tech.* **2010,** *44*, 865-873.

(4) Pöschl, U.; Shiraiwa, M. Multiphase Chemistry at the Atmosphere–Biosphere Interface Influencing Climate and Public Health in the Anthropocene. *Chem. Rev.* **2015,** *115*, 4440-4475.

(5) George, I. J.; Abbatt, J. P. Heterogeneous Oxidation of Atmospheric Aerosol Particles by Gas-Phase Radicals. *Nat. Chem.* **2010,** *2*, 713-22.

(6) Gligorovski, S.; Abbatt, J. P. D. An Indoor Chemical Cocktail. *Science* **2018,** *359*, 632-633.

(7) Ye, J.; Abbatt, J. P. D.; Chan, A. W. H. Novel Pathway of So2 Oxidation in the Atmosphere: Reactions with Monoterpene Ozonolysis Intermediates and Secondary Organic Aerosol. *Atmos. Chem. Phys. Discuss.* **2017,** *2017*, 1-35.

(8) Richards-Henderson, N. K.; Goldstein, A. H.; Wilson, K. R. Sulfur Dioxide Accelerates the Heterogeneous Oxidation Rate of Organic Aerosol by Hydroxyl Radicals. *Environ. Sci. and Tech.* **2016,** *50*, 3554-3561.

(9) Richards-Henderson, N. K.; Goldstein, A. H.; Wilson, K. R. Large Enhancement in the Heterogeneous Oxidation Rate of Organic Aerosols by Hydroxyl Radicals in the Presence of Nitric Oxide. *J. Phys. Chem. Lett.* **2015,** *6*, 4451-4455.

(10) Mauldin III, R. L.; Berndt, T.; Sipila, M.; Paasonen, P.; Petaja, T.; Kim, S.; Kurten, T.; Stratmann, F.; Kerminen, V. M.; Kulmala, M. A New Atmospherically Relevant Oxidant of Sulphur Dioxide. *Nature* **2012,** *488*, 193-196.

(11) Boy, M.; Mogensen, D.; Smolander, S.; Zhou, L.; Nieminen, T.; Paasonen, P.; Plass-Dülmer, C.; Sipilä, M.; Petäjä, T.; Mauldin, L., et al. Oxidation of So2 by Stabilized Criegee Intermediate (Sci) Radicals as a Crucial Source for Atmospheric Sulfuric Acid Concentrations. *Atmos. Chem. Phys.* **2013,** *13*, 3865-3879.

(12) Ehn, M.; Thornton, J. A.; Kleist, E.; Sipila, M.; Junninen, H.; Pullinen, I.; Springer, M.; Rubach, F.; Tillmann, R.; Lee, B., et al. A Large Source of Low-Volatility Secondary Organic Aerosol. *Nature* **2014,** *506*, 476-479.

(13) Sarwar, G.; Simon, H.; Fahey, K.; Mathur, R.; Goliff, W. S.; Stockwell, W. R. Impact of Sulfur Dioxide Oxidation by Stabilized Criegee Intermediate on Sulfate. *Atmos. Environ.* **2014,** *85*, 204-214.

(14) Welz, O.; Savee, J. D.; Osborn, D. L.; Vasu, S. S.; Percival, C. J.; Shallcross, D. E.; Taatjes, C. A. Direct Kinetic Measurements of Criegee Intermediate (Ch2oo) Formed by Reaction of Ch2i with O2. *Science* **2012,** *335*, 204-207.

(15) Taatjes, C. A.; Welz, O.; Eskola, A. J.; Savee, J. D.; Scheer, A. M.; Shallcross, D. E.; Rotavera, B.; Lee, E. P. F.; Dyke, J. M.; Mok, D. K. W., et al. Direct Measurements of Conformer-Dependent Reactivity of the Criegee Intermediate Ch3choo. *Science* **2013,** *340*, 177-180.

(16) Osborn, D. L.; Taatjes, C. A. The Physical Chemistry of Criegee Intermediates in the Gas Phase. *Int. Rev. Phys. Chem.* **2015,** *34*, 309-360.

(17) Chhantyal-Pun, R.; Welz, O.; Savee, J. D.; Eskola, A. J.; Lee, E. P. F.; Blacker, L.; Hill, H. R.; Ashcroft, M.; Khan, M. A. H.; Lloyd-Jones, G. C., et al. Direct Measurements of Unimolecular and Bimolecular Reaction Kinetics of the Criegee Intermediate (Ch3)2coo. *J. Phys. Chem. A* **2017,** *121*, 4-15.

(18) Huang, H.-L.; Chao, W.; Lin, J. J.-M. Kinetics of a Criegee Intermediate That Would Survive High Humidity and May Oxidize Atmospheric So2. *Proc. Natl. Acad. Sci. U.S.A.* **2015,** *112*, 10857-10862.

(19) Zhang, X.; Zhuang, G.; Chen, J.; Wang, Y.; Wang, X.; An, Z.; Zhang, P. Heterogeneous Reactions of Sulfur Dioxide on Typical Mineral Particles. *J. Phys. Chem. B* **2006,** *110*, 12588-12596.

(20) Park, J.; Jang, M.; Yu, Z. Heterogeneous Photo-Oxidation of So2 in the Presence of Two Different Mineral Dust Particles: Gobi and Arizona Dust. *Environ. Sci. and Tech.* **2017,** *51*, 9605-9613.

(21) Luria, M.; Sievering, H. Heterogeneous and Homogeneous Oxidation of So2 in the Remote Marine Atmosphere. *Atmos. Environ.* **1991,** *25*, 1489-1496.

(22) Li, L.; Chen, Z. M.; Zhang, Y. H.; Zhu, T.; Li, J. L.; Ding, J. Kinetics and Mechanism of Heterogeneous Oxidation of Sulfur Dioxide by Ozone on Surface of Calcium Carbonate. *Atmos. Chem. Phys.* **2006,** *6*, 2453-2464.

(23) Davis, D. D.; Prusazcyk, J.; Dwyer, M.; Kim, P. Stop-Flow Time-of-Flight Mass Spectrometry Kinetics Study. Reaction of Ozone with Nitrogen Dioxide and Sulfur Dioxide. *J. Phys. Chem.* **1974,** *78*, 1775-1779.

(24) Weschler, C. J. Roles of the Human Occupant in Indoor Chemistry. *Indoor Air* **2016,** *26*, 6-24.

(25) Milstone, L. M. Epidermal Desquamation. *Journal of Dermatological Science* **2004,** *36*, 131-140.

(26) Picardo, M.; Ottaviani, M.; Camera, E.; Mastrofrancesco, A. Sebaceous Gland Lipids. *Dermato-endocrinology* **2009,** *1*, 68-71.

(27) Wisthaler, A.; Weschler, C. J. Reactions of Ozone with Human Skin Lipids: Sources of Carbonyls, Dicarbonyls, and Hydroxycarbonyls in Indoor Air. *Proc. Natl. Acad. Sci. U.S.A.* **2010,** *107*, 6568-75.

(28) Tang, X.; Misztal, P. K.; Nazaroff, W. W.; Goldstein, A. H. Siloxanes Are the Most Abundant Volatile Organic Compound Emitted from Engineering Students in a Classroom. *Environ. Sci. and Tech. Lett.* **2015,** *2*, 303-307.

(29) Lakey, P. S. J.; Wisthaler, A.; Berkemeier, T.; Mikoviny, T.; Pöschl, U.; Shiraiwa, M. Chemical Kinetics of Multiphase Reactions between Ozone and Human Skin Lipids: Implications for Indoor Air Quality and Health Effects. *Indoor Air* **2017,** *27*, 816-828.

(30) Heine, N.; Houle, F. A.; Wilson, K. R. Connecting the Elementary Reaction Pathways of Criegee Intermediates to the Chemical Erosion of Squalene Interfaces During Ozonolysis. *Environ. Sci. and Tech.* **2017,** *51*, 13740-13748.

(31) Hinsberg, W. D., Houle, F. A. . Kinetiscope a Stochastic Kinetics Simulator. Available under a No-Cost License www.hinsberg.net/kinetiscope (accessed March 2018).

(32) Berndt, T.; Jokinen, T.; Mauldin, R. L.; Petäjä, T.; Herrmann, H.; Junninen, H.; Paasonen, P.; Worsnop, D. R.; Sipilä, M. Gas-Phase Ozonolysis of Selected Olefins: The Yield of Stabilized Criegee Intermediate and the Reactivity toward So2. *J. Phys. Chem. Lett.* **2012,** *3*, 2892-2896.

(33) Vereecken, L.; Harder, H.; Novelli, A. The Reactions of Criegee Intermediates with Alkenes, Ozone, and Carbonyl Oxides. *Phys. Chem. Chem. Phys.* **2014,** *16*, 4039-4049.

(34) Fendel, W.; Matter, D.; Burtscher, H.; Schmidt-Ott, A. Interaction between Carbon or Iron Aerosol Particles and Ozone. *Atmos. Environ.* **1995,** *29*, 967-973.

(35) Razumovskii, S. D.; Lisitsyn, D. M. Reactions of Ozone with Double Bonds in Polymer and Biosystem Chemistry. *Polymer Science Series A* **2008,** *50*, 1187-1197.

(36) Kirschenbaum, L. J.; Rueckberg, B. A Correlation of the Solubility of Water in Hydrocarbons as a Function of Temperature Based on the Corresponding Vapor Pressure of Pure Water. *Chemical Sciences Journal* **2013,** *2013*, 1-9.

(37) van Dam, M. H. H.; Lamine, A. S.; Roizard, D.; Lochon, P.; Roizard, C. Selective Sulfur Dioxide Removal Using Organic Solvents. *Industrial & Engineering Chemistry Research* **1997,** *36*, 4628-4637.

(38) Abercromby, D. C.; Tiley, P. F. 937. The Condensed Phases of Sulphur Trioxide. Part Ii. Vapour Pressure of the Liquid at Temperatures up to the Critical Point. *Journal of the Chemical Society (Resumed)* **1963**, 4902-4904.

(39) Wiegel, A. A.; Wilson, K. R.; Hinsberg, W. D.; Houle, F. A. Stochastic Methods for Aerosol Chemistry: A Compact Molecular Description of Functionalization and Fragmentation in the Heterogeneous Oxidation of Squalane Aerosol by Oh Radicals. *Phys. Chem. Chem. Phys.* **2015,** *17*, 4398-411.

(40) Karagulian, F.; Scott Lea, A.; Dilbeck, C. W.; Finlayson-Pitts, B. J. A New Mechanism for Ozonolysis of Unsaturated Organics on Solids: Phosphocholines on Nacl as a Model for Sea Salt Particles. *Phys. Chem. Chem. Phys.* **2008,** *10*, 528-541.

(41) Sheps, L. Absolute Ultraviolet Absorption Spectrum of a Criegee Intermediate Ch2oo. *J. Phys. Chem. Lett.* **2013,** *4*, 4201-4205.

(42) Stone, D.; Blitz, M.; Daubney, L.; Howes, N. U. M.; Seakins, P. Kinetics of Ch2oo Reactions with So2, No2, No, H2o and Ch3cho as a Function of Pressure. *Phys. Chem. Chem. Phys.* **2014,** *16*, 1139-1149.

(43) Liu, Y.; Bayes, K. D.; Sander, S. P. Measuring Rate Constants for Reactions of the Simplest Criegee Intermediate (Ch2oo) by Monitoring the Oh Radical. *J. Phys. Chem. A* **2014,** *118*, 741-747.

(44) Berndt, T.; Jokinen, T.; Sipilä, M.; Mauldin, R. L.; Herrmann, H.; Stratmann, F.; Junninen, H.; Kulmala, M. H2so4 Formation from the Gas-Phase Reaction of Stabilized Criegee Intermediates with So2: Influence of Water Vapour Content and Temperature. *Atmos. Environ.* **2014,** *89*, 603-612.

(45) Martinez, R. I.; Herron, J. T. Gas-Phase Reaction of So2 with a Criegee Intermediate in the Presence of Water Vapor. *Journal of Environmental Science and Health . Part A: Environmental Science and Engineering* **1981,** *16*, 623-636.

(46) Vereecken, L.; Harder, H.; Novelli, A. The Reaction of Criegee Intermediates with No, Ro2, and So2, and Their Fate in the Atmosphere. *Phys. Chem. Chem. Phys.* **2012,** *14*, 14682-14695.

(47) Newland, M. J.; Rickard, A. R.; Vereecken, L.; Muñoz, A.; Ródenas, M.; Bloss, W. J. Atmospheric Isoprene Ozonolysis: Impacts of Stabilised Criegee Intermediate Reactions with So₂, H₂O and Dimethyl Sulfide. *Atmos. Chem. Phys.* **2015,** *15*, 9521-9536.

(48) Shang, J.; Passananti, M.; Dupart, Y.; Ciuraru, R.; Tinel, L.; Rossignol, S.; Perrier, S.; Zhu, T.; George, C. So2 Uptake on Oleic Acid: A New Formation Pathway of Organosulfur Compounds in the Atmosphere. *Environ. Sci. and Tech. Lett.* **2016,** *3*, 67-72.

(49) Reiner, T.; Arnold, F. Laboratory Investigations of Gaseous Sulfuric Acid Formation Via So3+H2o+M→H2so4+M: Measurement of the Rate Constant and Product Identification. *J. Chem. Phys.* **1994,** *101*, 7399-7407.

(50) Berndt, T.; Böge, O.; Stratmann, F.; Heintzenberg, J.; Kulmala, M. Rapid Formation of Sulfuric Acid Particles at near-Atmospheric Conditions. *Science* **2005,** *307*, 698-700.

(51) Kulmala, M.; Vehkamäki, H.; Petäjä, T.; Dal Maso, M.; Lauri, A.; Kerminen, V. M.; Birmili, W.; McMurry, P. H. Formation and Growth Rates of Ultrafine Atmospheric Particles: A Review of Observations. *J. Aerosol Sci.* **2004,** *35*, 143-176.

(52) Fiedler, V.; Dal Maso, M.; Boy, M.; Aufmhoff, H.; Hoffmann, J.; Schuck, T.; Birmili, W.; Hanke, M.; Uecker, J.; Arnold, F., et al. The Contribution of Sulphuric Acid to Atmospheric Particle Formation and Growth: A Comparison between Boundary Layers in Northern and Central Europe. *Atmos. Chem. Phys.* **2005,** *5*, 1773-1785.

(53) Kuang, C.; McMurry, P. H.; McCormick, A. V.; Eisele, F. L. Dependence of Nucleation Rates on Sulfuric Acid Vapor Concentration in Diverse Atmospheric Locations. *J. Geophys. Res.: Atmos.* **2008,** *113*.

(54) Wiegel, A. A.; Wilson, K. R.; Hinsberg, W. D.; Houle, F. A. Stochastic Methods for Aerosol Chemistry: A Compact Molecular Description of Functionalization and Fragmentation in the Heterogeneous Oxidation of Squalane Aerosol by Oh Radicals. *PCCP* **2015,** *17*, 4398-4411.

(55) Kulmala, M.; Pirjola, L.; Mäkelä, J. M. Stable Sulphate Clusters as a Source of New Atmospheric Particles. *Nature* **2000,** *404*, 66.

(56) Vehkamäki, H.; Kulmala, M.; Napari, I.; Lehtinen, K. E. J.; Timmreck, C.; Noppel, M.; Laaksonen, A. An Improved Parameterization for Sulfuric Acid–Water Nucleation Rates for Tropospheric and Stratospheric Conditions. *J. Geophys. Res.: Atmos.* **2002,** *107*, 3-10.

(57) Benson, D. R.; Erupe, M. E.; Lee, S.-H. Laboratory-Measured H2so4-H2o-Nh3 Ternary Homogeneous Nucleation Rates: Initial Observations. *Geophys. Res. Lett.* **2009,** *36*, 1-6.

(58) Kurten, A.; Munch, S.; Rondo, L.; Bianchi, F.; Duplissy, J.; Jokinen, T.; Junninen, H.; Sarnela, N.; Schobesberger, S.; Simon, M., et al. Thermodynamics of the Formation of Sulfuric Acid Dimers in the Binary (H2so4-H2o) and Ternary (H2so4-H2o-Nh3) System. *Atmospheric Chemistry and Physics* **2015,** *15*, 10701-10721.

(59) Seow, W. J.; Downward, G. S.; Wei, H.; Rothman, N.; Reiss, B.; Xu, J.; Bassig, B. A.; Li, J.; He, J.; Hosgood, H. D., et al. Indoor Concentrations of Nitrogen Dioxide and Sulfur Dioxide from Burning Solid Fuels for Cooking and Heating in Yunnan Province, China. *Indoor Air* **2016,** *26*, 776-783.

(60) Brauer, M.; Henderson, S.; Kirkham, T.; Lee, K. S.; Rich, K.; Teschke, K. *Review of the Health Risks Associated with Nitrogen Dioxide Andsulfur Dioxide in Indoor Air.*; Report to Health Canada: 2002.